



Effects of Gamma Ray in Concrete After Low Dose

L. Bastos¹, O. de Araújo¹, T. Teixeira¹, S. Calixto², A. Machado¹, R. Funcke¹, M. Gonçalves², R. Lopes¹, D. Oliveira¹

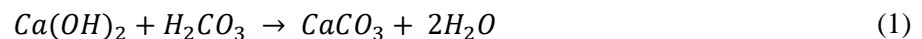
¹ *luanfbastos@gmail.com, olgaufjrjlin@gmail.com, tamara.porfiro@coppe.ufrj.br, alessandra.machado@coppe.ufrj.com, renatafuncke@gmail.com, rlopes@coppe.ufrj.br, davifoliveira@coppe.ufrj.br*
Nuclear Instrumentation Laboratory/PEN/COPPE/UFRJ

² *marcelogoncalves@ugb.edu.br, calixto.sebastiao.jr@gmail.com*
Geraldo di Biase University

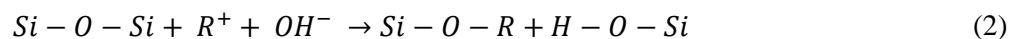
1. Introduction

Concrete is a composite material that consists essentially of a binding medium within which are embedded particles or fragments of aggregate [1] and is widely used in different ways such as structural, filling and shielding.

Carbonation is a phenomenon that occurs when carbon dioxide molecules penetrate the concrete structure through the existence of connected pores. When there are water molecules in the pores, a reaction can occur between them and carbon dioxide that generates carbonic acid. Carbonic acid reacts with the hydration products generating calcite and is demonstrated in equation 1. Although the presence of calcite increases mechanical properties, it causes a reduction in pH, which exposes steel bars through corrosion [2,3].



Carbonation can also occur when gamma radiation interacts with concrete. Gamma ray interacts with H₂O in pores and produces H⁺ and OH⁻, the first one goes to concrete surface, but OH⁻ participates in alkali-silica-reaction (A-S-R) and reduces micro pores and produces ions and free radicals. The reaction is demonstrated through equation 2, where R⁺ is Na⁺ or Ca⁺ [4].



Gamma rays change the internal structure of concrete in low doses and can cause deterioration if concrete interacts with doses higher than 100 kGy [3-7]. The aim of this work is to verify the modifications that occur in the concrete structure for three different traits with three fine aggregates by analyzing the porosity, and compressive strength after an irradiation of 10 kGy.

2. Methodology

The samples used in this study are sixty-three 100 mm x 50 mm (H x d) plugs, as determined in NBR 7215 standard [8], divided in three traits that are listed in table I. The IPT samples were prepared with standard sand as determined in NBR 7211 standard [9], the conventional samples were prepared using conventional sand that can be bought in any hardware store and the ART samples were prepared with artificial sand (gravel that can be classified as fine aggregate). It was used a 40 MPa concrete and a water cementing rate of 0.48. In order to study the effects of the radiation in the structure of the concrete samples, they were prepared for irradiation on a Gammacell irradiator with a 25.31 TBq Co⁶⁰ source. The measurements were performed in each type of sample for the control group (not irradiated) and

irradiated for 10 kGy.

Table I: Quantity of elements used in concrete samples.

Samples	Cement (g)	Standard Sand (g)	Conventional Sand (g)	Artificial Sand (g)
IPT	642	1872	-	-
ART	642	-	1872	-
Conventional	642	-	-	1872

MicroCT analyses were carried out using a Phoenix Vtomex|m GE system. The system is equipped with a microfocus X-ray tube with a maximum voltage of 300 kV and maximum power of 500 W. A 410 mm x 410 mm a-Si digital flat panel detector with a pixel size of 200 μm and a bit-depth of 14 bits was used to register the cone x-ray beam transmission. The parameters used in the scans were as follows: voltage of 165 kV, cathode current of 220 μA , and a voxel size of 60.8 μm . The samples were positioned in a perpendicular orientation to the X-rays beam and the projections were taken over 360° at angular steps of 0.2°. The acquisition time was of 250 ms/step and the integration was of 3 frames, with a skip of 2 frames between projections to reduce the afterglow effect. A 1.0 mm thick aluminum filter was used to reduce the contribution of low energy photons (beam hardening effect).

After the acquisition processes, the volume was reconstructed using the datos x reconstruction (Version 2.5.0) software. In order to quantify the porosity of the samples, the CTAn software (Version 1.18.4.0) was used to perform the image segmentation and after that, the quantitative analyses. The application of this technique is easily found in literature [10-13].

The mechanical test was performed using Contenco's hydraulic press. The maximum load capacity is 100 T and the maximum sample height is 145 mm. The mechanical test was performed when the samples reached 76 days. The test was performed for all samples and an average for compressive strength was determined.

3. Results and Discussion

The porosity of the samples, before and after gamma irradiation are shown in table II. It is possible to notice a significant variation for ART and IPT after a dose of 10 kGy. Porosity decreased by 13.83% for ART and 12.28% for IPT. The samples also demonstrated a variation in open pores, the principal way for natural carbonation. Decrease of porosity is explained by reactions that occur when gamma rays interact with water. The water is responsible to liberate OH^- that reacts with Na^+ and Ca^+ and promote changes in internal pores. Connectivity Density represents a degree of connectivity of trabecular pores normalized by the sample volume [14] and is important to notice how gamma rays affect the connected pores that allow the natural carbonation.

Table II: Pore Characteristic.

Samples	Porosity (%)		Open Pores (%)		Connectivity Density (mm^{-3})	
	0 kGy	10 kGy	0 kGy	10 kGy	0 kGy	10 kGy
ART	3.408	2.937	0.871	0.599	8×10^{-5}	5×10^{-5}
IPT	6.237	5.471	1.574	1.118	12×10^{-5}	7×10^{-5}
Conventional	5.994	5.695	1.600	1.348	9×10^{-5}	7×10^{-5}

Results for compressive strength are in table III. All samples had an increase in compressive strength. Conventional was the sample with smaller increase, but still significant (6.71%), and IPT was with greater

increase (12.07%). ART had an increase of about 7.64%.

These results were expected when table II is analyzed, because the porosity decreased when the samples interacted with gamma rays. When concrete is irradiated, the micro pores are filled up with the product of chemical reactions, like calcite, and had an increase in compressive strength and can be noticed when porosity is analyzed. H₂O molecules undergo chemical reactions and H⁺ leave the interior of the concrete in gaseous state, while OH⁻ reacts with different radicals and generates solid crystals. Thus, there is a substitution of material in liquid state for a material in solid state in the internal structure of concrete.

Table III: Mechanical Strength.

Samples	Compressive Strength (MPa)	
	0 kGy	10 kGy
ART	33.5	36.0
IPT	63.7	71.3
Conventional	39.3	42.0

4. Conclusions

Concrete irradiation can modify internal structure and MicroCT proved to be very useful to evaluate the change in the porosity. Decrease of porosity was expected by chemical reactions that occur, because the products promote carbonation. Compressive strength showed an increase after irradiation, this was expected when the porosity is analyzed. Although there is a desirable increase in the strength of concrete, this result must be viewed with caution, since chemical reactions that occur in concrete after incidence of gamma radiation cause carbonation, which makes the steel bars unprotected from external agents. Further studies are needed to evaluate how higher doses interfere with the properties presented by concrete.

Acknowledgements

This study was financed in part by the Coordenação de Aperfeiçoamento de Pessoal de Nível Superior - Brasil (CAPES) - Finance Code 001. The authors also would like to thank the Conselho Nacional de Desenvolvimento Científico e Tecnológico (CNPq) and Fundação de Amparo à Pesquisa do Estado do Rio de Janeiro (FAPERJ) for their financial support.

References

- [1] ASTM C125 - *Standard Terminology Relating to Concrete and Concrete Aggregates*, ASTM International, West Conshohocken, PA (2018).
- [2] Neville A. M., *Properties of Concrete*, 5 ed., Edimburgo, Pearson Education Limited (2011).
- [3] Vodák, F.; Vydra, V.; Trtík, K., et al., 2011, "Effect of gamma irradiation on properties of hardened cement paste", *Materials and Structures*, v. 44, pp. 101-107.
- [4] Rezaei Ochbelagh, D.; Azimkhani, S.; GasemzadehMosavinejad, H., "Effect of gamma and lead as an additive material on the resistance and strength of concrete", *Nuclear Engineering and Design*, v. 241, pp. 2359-2363 (2011).

- [5] Soo, P.; Milian, L. M., "The effect of gamma radiation on the strength of Portland cement mortars", *Journal of Materials Science Letters*, v 20, pp 1345-1348 (2001).
- [6] Bar-Nes, G.; Katz, A.; Peled, Y.; Zeiri, Y., "The combined effect of radiation and carbonation on the immobilization of Sr and Cs ions in cementitious pastes", *Materials and Structures*, v.41, pp. 1563-1570 (2008).
- [7] Zatloukalová, J.; Dewynter-Marty, V.; Zatloukal, J.; Kolár, K.; Bernachy-Barbe, F.; Bezdicka, P.; Konvalinka, P., "Microstructural and micro-mechanical property changes of cement pastes for ILW immobilization due to irradiation", *Journal of Nuclear Materials*, v. 540 (2020).
- [8] NBR 7215 - *Cimento Portland - Determinação da resistência à compressão de corpos de prova cilíndricos*, Associação Brasileira de Normas Técnicas (2019).
- [9] NBR 7211 - *Agregados para concreto - Especificação*, Associação Brasileira de Normas Técnicas (2009).
- [10] Machado, A.S.; Oliveira, D.F.; Gama Filho, H.S.; Latini, R.; Bellido, A.V.B.; Assis, J.T.; Anjos, M.J.; Lopes, R.T., "Archeological ceramic artifacts characterization through computed microtomography and x-ray fluorescence", *X Ray Spectrom.*, v. 46, pp. 427–434 (2017).
- [11] Oliveira, D.F.; Santos, R.S.; Machado, A.S.; Silva, A.S.S.; Anjos, M.J; Lopes, R.T., "Characterization of scale deposition in oil pipelines through X-Ray Microfluorescence and X-Ray microtomography", *Applied Radiation and Isotopes*, v. 151, pp. 247-255 (2019).
- [12] Bastos, L.F.; de Araújo, O.M.O.; Machado, A.S.; Oliveira, D.F.; Lopes, R.T., "X-Ray Microtomography System Applied in Characterization of Lightweight Concrete Structures", *ASME Journal of Nondestructive Evaluation*, v. 3(4) (2020).
- [13] Ferreira, C.G.; Lopes, R.T.; dos Santos, T.M.P.; Oliveira, D.F.; Martins, F.D.F.; Pereira, G.R., "Non-destructive inspection of laminated pipe joints in polymeric composite material reinforced by fiberglass", *Nucl. Instrum. Methods Phys. Res., Sect. A*, v. 954 (2020).
- [14] Bouxsein, M. L.; Boyd, S. K.; Christiansen, B. A.; Guldborg, R. E.; Jepsen, K. J.; Muller, R., "Guidelines for Assessment of Bone Microstructure in Rodents Using Micro-Computed Tomography", *Journal of Bone and Mineral Research*, v.25(7), pp. 1468-1486 (2010).